Thermal Regulation of Methane Hydrate Dissociation: Implications for Gas Production Models

Susan Circone, Stephen H. Kirby, and Laura A. Stern*

U.S. Geological Survey, 345 Middlefield Road MS 977, Menlo Park, California 94025

Received February 17, 2005. Revised Manuscript Received September 12, 2005

Thermal self-regulation of methane hydrate dissociation at pressure, temperature conditions along phase boundaries, illustrated by experiment in this report, is a significant effect with potential relevance to gas production from gas hydrate. In surroundings maintained at temperatures above the ice melting point, the temperature in the vicinity of dissociating methane hydrate will decrease because heat flow is insufficient to balance the heat absorbed by the endothermic reaction: $CH_4{\cdot}nH_2O$ (s) = CH_4 (g) + nH_2O (l). Temperature decreases until either all of the hydrate dissociates or a phase boundary is reached. At pressures above the quadruple point, the temperature-limiting phase boundary is that of the dissociation reaction itself. At lower pressures, the minimum temperature is limited by the H_2O solid/liquid boundary. This change in the temperature-limiting phase boundary constrains the pressure, temperature conditions of the quadruple point for the CH_4-H_2O system to 2.55 ± 0.02 MPa and 272.85 ± 0.03 K. At pressures below the quadruple point, hydrate dissociation proceeds as the liquid H_2O produced by dissociation freezes. In the laboratory experiments, dissociation is not impeded by the formation of ice byproduct per se; instead rates are proportional to the heat flow from the surroundings. This is in contrast to the extremely slow dissociation rates observed when surrounding temperatures are below the H_2O solid/liquid boundary, where no liquid water is present. This "anomalous" or "self" preservation behavior, most pronounced near 268 K, cannot be accessed when surrounding temperatures are above the H_2O solid/liquid boundary.

Introduction

Huge reservoirs of methane, stored in the form of gas hydrate, have been estimated to exist in sediments on continental margins and in arctic permafrost zones.[1] Natural gas recovery from these hydrate-bearing deposits, in particular from arctic permafrost, is a potentially viable, economical source for methane gas.[2−5] In recovering natural gas from a conventional reservoir, gas flow is driven by the pressure difference between the reservoir and the recovery point and depends on host rock permeability. Gas production from hydrate-bearing sediments requires the additional, energetically costly step of hydrate dissociation achieved by (1) altering the in situ conditions such that the gas hydrate is no longer stable, and (2) maintaining pressure, temperature (*P*, *T*) conditions such that dissociation continues at an economically productive rate.

During dissociation, methane gas is released by the reaction:

$$CH_4{\cdot}nH_2O\ (s) = CH_4\ (g) + nH_2O\ (l) \qquad (1)$$

and can be achieved by three methods, either singly or in combination: (1) decreasing pressure, (2) increasing temperature, or (3) introducing a chemical inhibitor (Figure 1). All three methods alter conditions such that hydrate is no longer thermodynamically stable, either by moving conditions outside the hydrate stability boundary (1 and 2) or by shifting the stability boundary itself by lowering the chemical activity of water (3). Pressure reduction has been shown to be the most economical method[2] for recovering natural gas from hydrate, but it is still more costly than recovering free gas from below the hydrate-bearing zone, in which case hydrate dissociation may supplement gas production. Regardless of the method used, there will be a thermal response once dissociation begins because hydrate dissociation requires heat to proceed. Heat conduction, in particular through a porous medium such as may occur in a permafrost setting, will be insufficient to maintain isothermal conditions, and the temperature of the system will decrease rapidly. The thermal evolution of the system will depend on several factors, including the level of hydrate saturation, whether pressure is fixed or continuously changing, and whether advection of warm fluids contributes to the heat flow into the system. In settings where the hydrate saturation is low, all of the hydrate may dissociate before *P*, *T* conditions reach a limiting phase boundary (this will depend on the level of saturation and the starting temperature offset above

* Corresponding author. Telephone: (650) 329-4811. Fax: (650) 329-5163. E-mail: lstern@usgs.gov.

(1) Kvenvolden, K. A. *Chem. Geol.* **1988**, *71*, 41−51.
(2) Sloan, E. D. *Clathrate Hydrates of Natural Gases*, 2nd ed.; Marcel Dekker: New York, 1998; 705 p.
(3) Collett, T. S. *AAPG Bull.* **2002**, *86*, 1971−1992.
(4) Moridis, G. J.; Collett, T. In *Recent Advances in the Study of Gas Hydrates*; Taylor, C., Qwan, J., Eds.; Kluwer Academic/Plenum Publishers: Norwell, MA, 2004; pp 75−88.
(5) Moridis, G. J.; Collett, T.; Dallimore, S.; Satoh, T.; Hancock, S.; Weatherhill, B. *J. Pet. Sci. Eng.* **2004**, *43*, 219−239.

10.1021/ef0500437 CCC: $30.25
Published on Web 00/00/0000 PAGE EST: 6.1

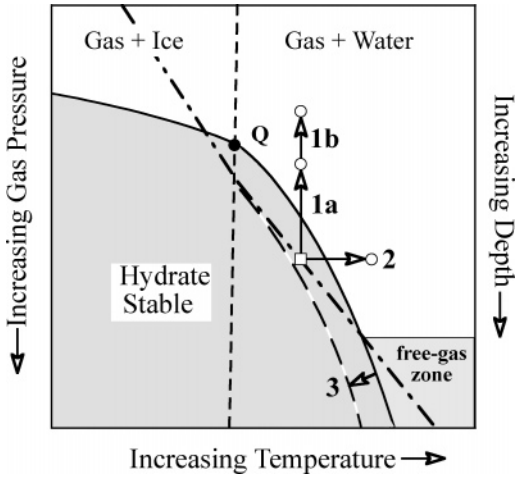

Figure 1. Schematic phase diagram of the CH_4-H_2O system in a geologic context (with pressure and depth increasing downward), showing the hydrate stability boundary (solid line), the H_2O solid/liquid boundary (dashed line), the quadruple point (**Q**) at the intersection of these two boundaries, and a typical geothermal gradient in a permafrost zone (dash−dot line) that intersects the methane hydrate stability field. Three possible methods for promoting in situ gas hydrate dissociation for natural gas production are also shown: (1) depressurization, (2) thermal stimulation, and (3) injection of a chemical inhibitor that shifts the stability boundary to lower temperatures (long dashed line). The starting condition is indicated by □, and the new P, T conditions for pathways 1 and 2 are indicated by ○. Trapped gas can also be recovered from the free gas zone, defined at the lower intersection of the geothermal gradient with the hydrate stability boundary.

the hydrate + water + gas equilibrium boundary). However, in more hydrate-rich settings, temperature in the vicinity of the dissociating hydrate will decrease and may become temporarily fixed at a phase boundary during dissociation. In this case, thermal self-regulation can occur, provided that the P, T conditions of the surroundings remain outside the hydrate stability field.

We have observed several aspects of thermal self-regulation during hydrate dissociation in isobaric laboratory experiments conducted on pure methane hydrate at temperatures above 273 K.[6−8] Dissociation rates are proportional to the heat flow from the surroundings, increasing with the temperature difference between the surroundings and the limiting phase boundary at that pressure. In these earlier experiments, pressure remained constant as dissociation proceeded by allowing the released gas to escape, and the effect of changing pressure conditions was not investigated. In the present study, we monitor hydrate dissociation at a range of pressures spanning the quadruple point (**Q**), the pressure, temperature condition at which the hydrate phase boundary intersects the ice/water phase boundary, where hydrate, methane gas, ice, and water coexist in equilibrium (Figure 1). Results from this experiment are compared to the previously published isobaric data on synthetic methane hydrate, as well as field observations of dissociating hydrate in recovered drill core samples. The observed behavior is in marked contrast to the extremely $P-T$ path-dependent dissociation behavior exhibited by methane hydrate at temperatures below 273 K.[9,10] Thermal self-regulation can significantly affect local environmental conditions during hydrate dissociation, and the resulting thermal boundary constraints imposed by phase equilibria, in particular at pressures below the quadruple point, should be included in gas production models.

Experimental Methods

The dissociation experiment was performed on a pure, porous synthetic sample of methane hydrate with a nominal intergranular porosity of 30%. Methane hydrate was synthesized from pressurized CH_4 gas and granular H_2O ice using the method described by Stern et al.,[9,11] in which reactants are heated from 250 K to holding conditions of 290 K, 30 ± 3 MPa and maintained for several hours. The complete conversion of ice to hydrate plus excess methane gas was confirmed prior to the dissociation experiment reported here. The methane hydrate sample, formed from 26.0 g of ice in a 2.54 cm × 10 cm long pressure cylinder, had an as-synthesized composition of $CH_4 \cdot 5.9H_2O$.[12]

Dissociation was monitored using our custom-built flow meter,[12] in which released gas is collected at 0.1 MPa. Gas release is determined by monitoring the change in weight of an inverted, H_2O-filled, close-ended cylinder as released gas displaces the H_2O. Measured gas yields have an uncertainty of ±1%.[12] We controlled the pressure in the sample vessel to within ±0.03 MPa of the set point pressure using a back pressure regulator (Tescom model ER 3000), situated between the sample pressure vessel and the flow meter, that released gas to the flow meter as the hydrate dissociated (Figure 2). Pressure is monitored continuously with a pressure transducer that was calibrated to a digital Heise gauge (model ST-2H). Note that the use of trade, product, industry, or firm names in this report is for descriptive purposes only and does not constitute endorsement by the U.S. Government.

The d-limonene bath surrounding the sample pressure vessel was maintained at constant temperatures to within ±0.002 K by a precision Hart standard bath (model 7081-CSI), and temperature was measured independently to within ±0.006 K using a Hart platinum resistance thermometer (PRT, model 5627-12, attached to a Hart 1502A electronic box). The internal temperature of the hydrate sample (T_{sample}) was monitored during the experiment using a radially and axially centered chromel−alumel (Type K) thermocouple, referenced to a Hart Scientific Zero Point Calibrator (model 9101). Sample temperature is typically accurate to ±0.1 K at 0.1 MPa, with a precision of ±0.03 K. However, we were able to improve accuracy to ±0.03 K by calibrating the thermocouple to the high-precision bath PRT under conditions of constant T and no hydrate dissociation. In experiments in which four thermocouples were used to measure interior and near-surface sample temperatures,[6−8] sample temperature is uniform during dissociation. Temperature rises once hydrate dissociation is complete at a particular thermocouple location, typically rising last at the sample middle (location shown in Figure 2).

The dissociation experiment was performed in a sequence of five main stages (***I*−*V***, Figure 3). The sample was thermally

(6) Circone, S.; Stern, L. A.; Kirby, S. H.; Pinkston, J. C.; Durham, W. B. In *Gas Hydrates: Challenges for the Future*; Holder, G., Bishnoi, P., Eds.; New York Academy of Sciences: New York, 2000; pp 544−555.
(7) Circone, S.; Stern, L. A.; Kirby, S. H. *J. Phys. Chem. B* **2004**, *108*, 5747−5755.
(8) Circone, S.; Stern, L. A.; Kirby, S. H. *Am. Mineral.* **2004**, *89*, 1192−1201.
(9) Stern, L. A.; Circone, S.; Kirby, S. H.; Durham, W. B. *J. Phys. Chem. B* **2001**, *105*, 1756−1762.
(10) Stern, L. A.; Circone, S.; Kirby, S. H.; Durham, W. B. *Can. J. Phys.* **2003**, *81*, 271−283.
(11) Stern, L. A.; Kirby, S. H.; Durham, W. B. *Science* **1996**, *273*, 1843−1848.
(12) Circone, S.; Kirby, S. H.; Pinkston, J. C.; Stern, L. A. *Rev. Sci. Instrum.* **2001**, *72*, 2709−2716.

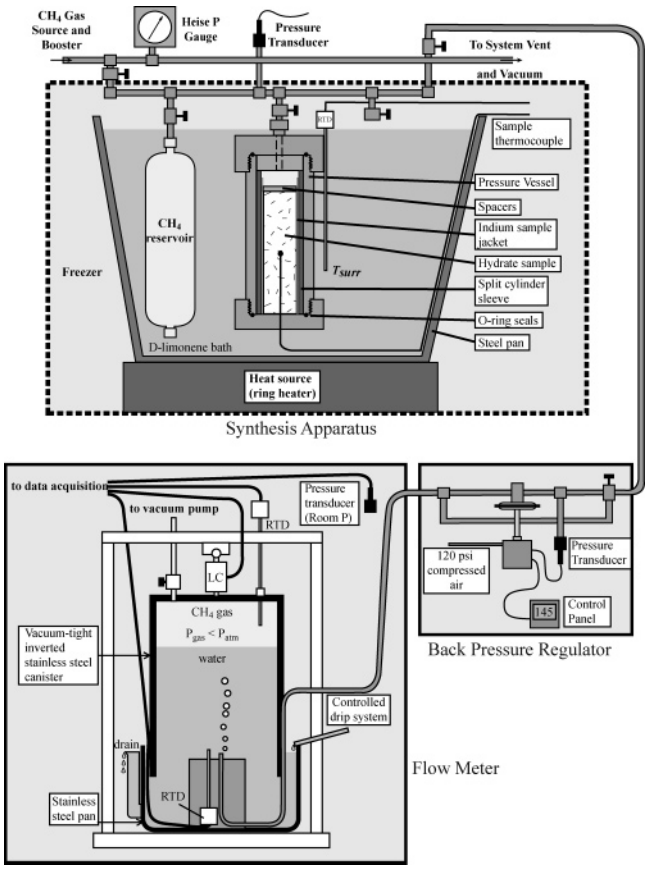

Figure 2. Schematic diagram (not to scale) of hydrate synthesis apparatus, back pressure regulator, and flow meter apparatus. A thermocouple, centered axially and radially in the hydrate sample, measures T_{sample}. The back pressure regulator maintains a constant, elevated pressure on the sample, while the flow meter operates at 0.1 MPa (see text; modified from Figure 1 in Circone et al.[8])

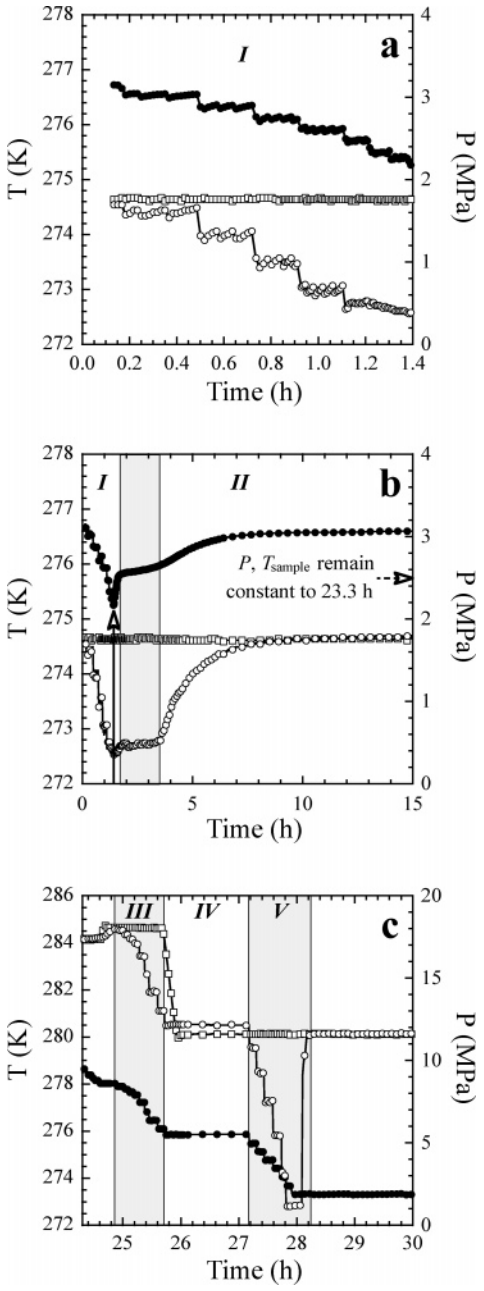

Figure 3. *P*, *T* record of the methane hydrate dissociation experiment, showing the history of depressurization (stages ***I***, ***III***, and ***V***), pressure rebound (stage ***II***), and bath cooling (stage ***IV***). Pressure (●), bath temperature (T_{surr}, □), and sample temperature (T_{sample}, ○) are plotted. All data points are plotted in (a), and every fifth data point is plotted in (b) and (c). The shaded region in (b) indicates the time interval during which *P*, T_{sample} conditions were approximately constant but T_{sample} was well below T_{surr} (see text). The arrow indicates the end of stage ***I*** and the beginning of stage ***II***. The shaded regions in (c) indicate the various stages of the experiment.

equilibrated at 274.65 K, and then pressure was lowered from 21.5 to 3.15 MPa. After the sample cooled due to adiabatic expansion of the free methane gas (not shown), the T_{sample} rebounded to 274.54 K and monitoring of dissociation began. As the bath temperature (T_{surr}) was held constant at 274.65 K, pressure was decreased in steps. The sample temperature response and the gas released by dissociation (not shown) were monitored (stage ***I***, Figure 3a). After 1.4 h, the sample was isolated from the back pressure regulator while T_{surr} remained isothermal (arrow, Figure 3b). The pressure and sample temperature rose over the next 8 h to 3.07 MPa, 274.65 K and remained constant for the next 13 h (stage ***II***, Figure 3b). At this point, the pressure was raised to 9.6 MPa, then the bath temperature was raised first to 284.15 K, then to 284.65 K. Once the sample thermally equilibrated with T_{surr}, pressure was decreased in steps to 5.51 MPa (stage ***III***, Figure 3c). The bath temperature was then decreased to 280.15 K (stage ***IV***, Figure 3c). In the final stage of the experiment (stage ***V***, Figure 3c), pressure was again decreased in steps to 1.90 MPa.

Results and Discussion

Using the procedure described above, the pressure on the methane hydrate sample, maintained in isothermal surroundings, was decreased in a stepwise manner. The thermal response of the sample, as well as the occurrence and rate of dissociation, were monitored at a variety of *P*, *T* conditions. During stage ***I***, T_{sample} became increasingly depressed below T_{surr} (Figure 3a) with each pressure decrease, and the rate of dissociation generally increased (Figure 4). The sudden increase in dissociation rate at 1.15 h corresponded to the point at which *P* was first decreased below the quadruple point. At the beginning of stage ***II***, we isolated the sample from the back pressure regulator such that no gas was released to the flow meter. Pressure and T_{sample} climbed (Figure 3b) over the next 8 h as dissociation continued until conditions reached 3.07 MPa, 274.65 K. During this stage, *P*, T_{sample} conditions stalled near 2.6 MPa, 272.7 K for almost 2 h (shaded region, Figure 3b). During

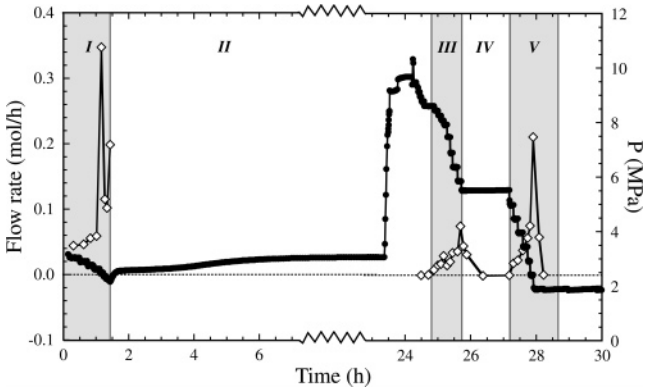

Figure 4. Dissociation rates (◇) and pressures (●) measured during stages ***I***, ***III***, ***IV***, and ***V***. Dissociation was not monitored during stage ***II***, as the sample was isolated from the flow meter. Following a depressurization step, dissociation rates were calculated from the net release of gas[12] accrued over a time interval in which P, T_{sample} conditions were constant (rate uncertainties on the order of 1.5%). See text for discussion of the observed dissociation rates.

stage ***III*** (Figure 3c, Figure 4), we resumed the stepwise decrease of pressure starting from the new P, T conditions, and the dissociation rate increased and T_{sample} decreased with each pressure decrease. During stage ***IV***, dissociation slowed and then stalled after we decreased T_{surr} to below the sample temperature of 280.65 K. We resumed decreasing pressure during stage ***V***. T_{sample} again decreased in steps, and the dissociation rate increased until 28.1 h, when dissociation was complete. The system then returned to thermal equilibrium within minutes.

The response of the hydrate sample to the various P, T conditions imposed in stages ***I***−***V*** is consistent with the phase equilibria of the CH_4−H_2O system (Figure 5). In stages ***I***, ***III***, and ***V***, pressure was decreased until conditions lay outside the methane hydrate stability field, and dissociation began. As pressure was decreased further (Figure 5a,c), T_{sample} decreased, maintaining sample conditions on the hydrate stability boundary. When we dropped the pressure below the quadruple point in stages ***I*** and ***V***, T_{sample} continued to decrease slightly but no longer followed the hydrate stability boundary, and instead followed a path subparallel to the H_2O solid/liquid boundary. This change in temperature behavior corresponds to the spikes in dissociation rates shown in Figure 4. As the pressure rebounded in stage ***II*** (Figure 5b), the sample conditions essentially retraced the P, T pathway followed in stage ***I***. As noted previously, conditions stalled for several hours near 2.6 MPa, 272.7 K. These P, T conditions differ by a few tenths of a degree from the H_2O solid/liquid boundary (273.0 K at 2.6 MPa), which defines the melting point of pure H_2O and neglects the effect of dissolved methane gas in the water. The presence of dissolved methane lowers the activity of the H_2O liquid phase relative to that of the solid, resulting in the depression of the H_2O freezing point. We calculated the equilibrium concentration of dissolved CH_4 (aq) in solution at P, T conditions of the H_2O solid/liquid boundary using the Henry's Law constants tabulated in Sloan,[2] while simultaneously solving for the freezing point depression for that amount of CH_4 (aq). Thus, we determined the position of the H_2O solid/aqueous solution equilibrium boundary shown

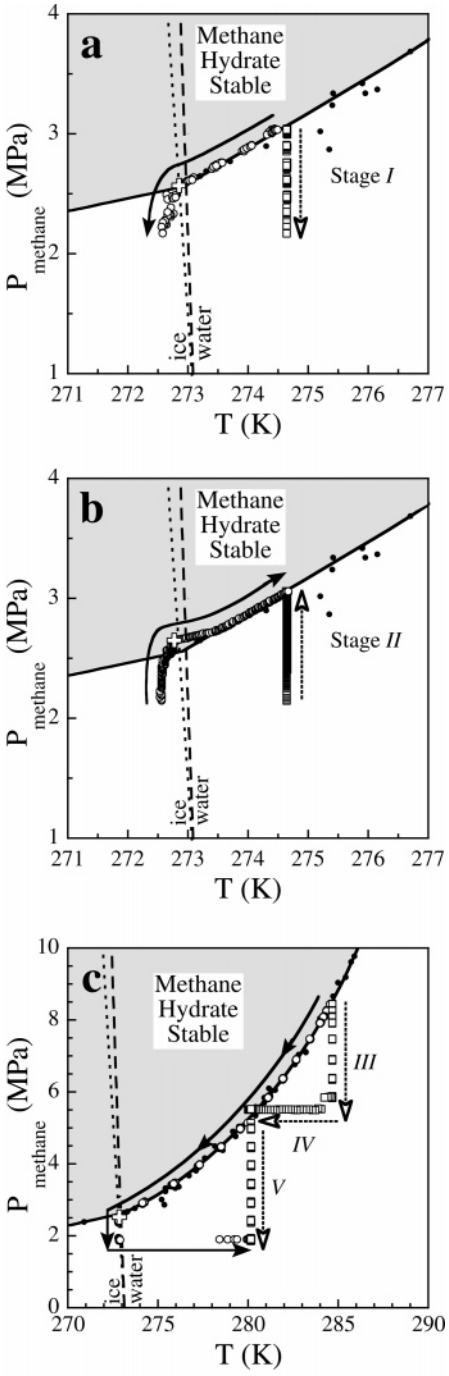

Figure 5. P, T conditions of the dissociation experiment shown with respect to the phase equilibria of the CH_4−H_2O system. Published phase equilibria data (●),[1] the hydrate stability boundary (solid line), the pure H_2O solid/liquid boundary (dashed line), and the H_2O solid/aqueous solution boundary (dotted line) are shown. The temperatures of the surrounding bath (□) and the hydrate (○) are plotted, with the open arrows indicating the directions of change for independent variables P or T_{surr}, and the solid arrow indicating the direction of change of the T_{sample} in response to pressure changes. The location of the quadruple point, determined by the break in slope of T_{sample}, is also shown (open plus sign, see text).

by the dotted line in Figure 5. Note that T_{sample} in stages ***I***, ***II***, and ***V*** is below this equilibrium boundary (see discussion below and ref 7).

The thermal responses described in this experiment have been observed previously in dissociation experi-

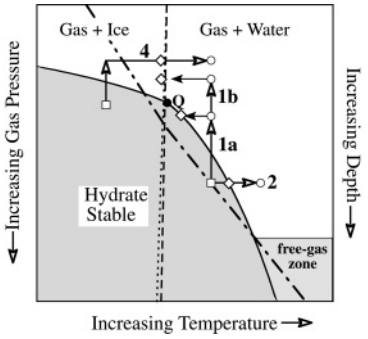

Figure 6. Schematic phase diagram of the CH_4-H_2O system in a geologic context (with pressure and depth increasing downward), showing the hydrate stability boundary (solid line), the pure H_2O solid/liquid boundary (dashed line), the H_2O solid/aqueous solution boundary (dotted line), the quadruple point (**Q**) at the intersection of these two boundaries, and a geothermal gradient in a permafrost zone (dash−dot line) that intersects the methane hydrate stability field. Starting conditions for the hydrate (□) and the *P*, *T* pathways followed to achieve hydrate dissociation are indicated by open arrows to the new *P*, *T* conditions (○): (1) depressurization to pressures either above (1a) or below (1b) the quadruple point, (2) thermal stimulation, and (4) low T_{surr} depressurization to below P_Q, followed by heating of the surroundings to a temperature above the H_2O solid/liquid boundary. The hydrate temperature (◊) becomes fixed on one of the phase boundaries, either stalling during heating (pathways 2 and 4) or decreasing (pathway 1, solid arrows) as dissociation proceeds.

ments on methane and other hydrates.[6−8] In those experiments, hydrate dissociation was achieved by following a variety of pathways, with T_{sample} becoming fixed on the same phase boundaries (Figure 6): (1) decreasing to a fixed *P* outside the hydrate stability field while T_{surr} was fixed at a temperature above the H_2O melting point (pathways 1a and 1b),[6,8] (2) heating the bath at a fixed *P* above P_Q to conditions outside the methane hydrate stability field (pathway 2),[13] and (3) after depressurizing a sample to below P_Q with T_{surr} below the H_2O melting point, warming T_{surr} above the melting point at a fixed *P* (pathway 4).[7−9] Furthermore, following pathway 1b, we have shown that hydrate + seawater ± quartz sand samples behave similarly, with temperatures depressed even further due to the presence of dissolved salts.[7] Pathway 3, injection of a chemical inhibitor, is not covered by our experimental results.

Similar behavior has been observed in dissociating samples of naturally occurring gas hydrates. Partial dissociation of hydrate often occurs during recovery of hydrate-bearing cores, as *P*, *T* conditions move outside the limit of hydrate stability. Interestingly, recovered hydrate-bearing marine sediment cores are often colder than any temperature encountered in situ or during retrieval (e.g., Leg 146, Site 889B;[14,15] Leg 201, Site 1230;[16] Leg 204, all sites),[17] and some cores have contained ice (e.g., Leg 164, Sites 996E and possibly 995A).[18] These thermal depressions can be several degrees and are used to infer the presence of hydrate and to identify core sections for further investigation. Because adiabatic expansion of free gases in sediment pores can also produce thermal depression signatures, the in situ presence of hydrate is confirmed by either direct observation or indicated by the "freshening" of pore waters in the core.

Thermal self-regulation during hydrate dissociation can be summarized as follows. When dissociation occurs at pressures above P_Q, and thus in the liquid H_2O stability field, the hydrate temperature becomes fixed at the hydrate stability boundary as dissociation proceeds (Figure 6).[13] During heating (pathway 2), for example, by injection of a high-temperature fluid, dissociation starts once the boundary is reached and will continue as long as sufficient heat is provided to the system. Upon depressurization (pathway 1a), hydrate dissociation begins and the hydrate temperature decreases until the hydrate boundary conditions are reached (Figure 5). Dissociation proceeds to completion at these fixed *P*, T_{sample} conditions. In both cases, the described behavior assumes that gas released by dissociation is free to flow and thus that pressure is not allowed to build (as it did intentionally in stage ***II***). In natural systems, this scenario is more likely to occur in a very permeable medium such as a permafrost deposit than in a marine environment, although other factors may affect permeability over the course of dissociation. At pressures below P_Q, depressurization along pathway 1b follows much the same progression; however, hydrate temperatures become fixed as much as 1−2 K below the H_2O melting point as dissociation proceeds to completion. This thermal regulation behavior is independent of T_{surr} and is consistent with that observed when partially dissociated hydrate is warmed to a temperature above the H_2O melting point (pathway 4). Again, *P*, *T* conditions become fixed at temperatures demonstrably below the H_2O ice/liquid boundary until dissociation proceeds to completion.[7]

The thermal response of the dissociating hydrate, in which T_{sample} decreases until conditions lie on a phase boundary, occurs because: (1) the dissociation reaction is endothermic, (2) there is sufficient hydrate present such that the enthalpy required to dissociate the hydrate is greater than the amount of latent heat released as hydrate (± sediment) cools, and (3) heat flow from the surroundings is insufficient to maintain thermal equilibrium. Above P_Q, thermal regulation occurs, and sample *P*, *T* conditions cannot drop below the hydrate stability boundary, as required by the phase rule:

$$F = C - P + 2 \qquad (2)$$

where *F* is the degrees of freedom, *C* is the number of components (two: CH_4 and H_2O), and *P* is the number of phases. In the case of the hydrate stability boundary, three phases are present: vapor (CH_4 + minor H_2O), solution (H_2O with dissolved CH_4), and solid methane

(13) Circone, S.; Kirby, S. H.; Stern, L. A. *J. Phys. Chem. B* **2005**, *109*, 9468−9475.
(14) Westbrook, G. K.; Carson, B.; Musgrave, R. J.; et al. *Proc. Ocean Drill. Program: Initial Rep.* **1994**, *146*.
(15) Kastner, M.; Kvenvolden, K. A.; Whiticar, M. J.; Camerlenghi, A.; Lorenson, T. D. *Proc. Ocean Drill. Program: Sci. Results* **1995**, *146*, 175−187.
(16) D'Hondt, S. L.; Jørgensen, B. B.; Miller, D. J.; et al. *Proc. Ocean Drill. Program: Initial Rep.* **2003**, *201*.
(17) Tréhu, A. M.; Bohrmann, G.; Rack, F. R.; Torres, M. E.; et al. *Proc. Ocean Drill. Program: Initial Rep.* **2003**, *204*.
(18) Paull, C. K.; Matsumoto, R.; Wallace, P. J.; et al. *Proc. Ocean Drill. Program: Initial Rep.* **1996**, *164*.

hydrate. Along the boundary there is one degree of freedom, meaning that only P or T_{sample} can be varied independently (in this experiment P was independent, fixing T_{sample}), and, to move away from the boundary, one phase must disappear. Thus, in stages ***I***, ***III***, and ***V***, we observed the decrease in T_{sample} along the boundary as pressure was decreased during hydrate dissociation.

The behavior at pressures below $P_{\mathbf{Q}}$, where sample conditions follow a pathway subparallel to the H_2O solid/liquid boundary, is not expected from inspection of the equilibrium phase diagram, but is wholly consistent with earlier isobaric dissociation results.[6−8] Thermal regulation at temperatures just below this phase boundary occurs regardless of pressure, T_{surr}, or dissociation rate in these experiments. At fixed P and T_{surr} conditions, the buffering temperature increases slightly as dissociation proceeds, and the temperature range depends on the dissociation rate and the composition of the hydrate-forming gas.[7] Based on several lines of evidence, including phase equilibria, experimental measurement, and direct observation of ice product following dissociation, we proposed[7] that hydrate is dissociating to CH_4 (g) and H_2O (l), which immediately freezes. The enthalpy released from freezing offsets the higher enthalpy needed to form the water product (by an additional n times 6.01 kJ/mol for $CH_4 \cdot nH_2O$). The hydrate temperature is depressed below the pure H_2O melting point due to the presence of dissolved gas in the water product prior to freezing. Melting point depression arises because the chemical potential of water is lowered by the presence of a dissolved species (methane gas) that is insoluble in the solid ice phase. Gas concentrations calculated from the observed freezing point depressions are between the equilibrium gas solubility (described above) and the concentration in the gas hydrate itself. Furthermore, the buffering temperature is lower for gases with higher equilibrium solubility (i.e., CO_2 vs methane, ethane, and propane; see ref 7 for further discussion).

This hypothesis is also consistent with the phase rule, in that the data points subparallel to the H_2O solid/liquid boundary (Figure 5, at P below the quadruple point) are in fact an extension of the invariant quadruple point. At the quadruple point, four phases coexist: vapor (CH_4 + minor H_2O), solid H_2O, solution (H_2O with dissolved CH_4), and solid methane hydrate. Thus, there are no degrees of freedom ($F = 2 - 4 + 2 = 0$). Under the conditions of the experiment, P and T_{sample} will remain fixed until one phase disappears, either hydrate or H_2O (s). Once all of the hydrate dissociates, P, T_{sample} conditions then become fixed at the pure H_2O melting point until all of the ice melts,[7] before T_{sample} finally rebounds to T_{surr}. During stage ***II*** (Figure 3b), we noted that approximately constant P and T_{sample} conditions arose, lasting for almost 2 h (shaded region). We surmise that during this interval, H_2O ice was melting even as dissociation continued, and once complete, P, T_{sample} conditions again rose sharply as one degree of freedom was regained. The approximately constant P, T_{sample} conditions, when plotted in Figure 5b, are located within the hydrate stability field at sample temperatures below the H_2O solid/aqueous solution boundary. The small pressure overstep of the hydrate boundary may be an artifact related to the large size of our hydrate sample. Regions of the sample nearer the vessel walls and away from the sample middle may pass through the quadruple point first, allowing the pressure to continue to rise slowly in this interval.

The location of the quadruple point **Q** is indicated by the break in slope of the P, T_{sample} conditions. Under decreasing pressure conditions, we locate **Q** at 272.85 K and 2.57 MPa (Figure 5a) or 272.85 K and 2.53 MPa (Figure 5c), consistent with the calculated position of the equilibrium H_2O solid/aqueous solution boundary. These values are also consistent with the tabulated value of 272.9 K and 2.563 MPa in Sloan.[1] An early phase equilibria study placed an equilibrium point for CH_4 (g) + H_2O (l) + methane hydrate at 273.15 K, 2.64 MPa,[19] also consistent with our results. Under increasing pressure conditions (Figure 5b), the break in slope is located at 272.77 K and 2.65 MPa. This measured difference in the inferred location of **Q**, at slightly higher P and lower T, exceeds our measurement uncertainties, but may be an artifact of the large sample size, as noted above. We deem the location of **Q** during stepwise pressure reduction, where the sample is responding rapidly to the changing conditions, a more reliable means of locating **Q**.

Conclusions

Thermal self-regulation arises during hydrate dissociation because the reaction requires heat to proceed, a requirement that drives the temperature of the dissociating hydrate down until a phase boundary is intersected, where temperature then follows the phase boundary as long as dissociation continues. This thermal response and the phase equilibria behind it expresses itself in interesting ways that are potentially important for natural-gas production from hydrates. Specifically, at pressures below the quadruple point, dissociation in warm surroundings will follow a thermal boundary just below the pure H_2O solid/liquid boundary. The dissociation reaction hydrate → gas + ice cannot be accessed along this pathway, unless the surroundings are cooled below the H_2O solid/liquid boundary or depressurization begins at thermal conditions below this boundary. In such cases, models would contend with the regime of anomalously slow dissociation rates for methane hydrate.[8−10]

Thermal self-regulation at the warm temperatures described in this paper results in a temperature minimum during hydrate dissociation and constrains the conditions under which dissociation proceeds. However, our experimental system is far simpler than that encountered in a natural setting. For example, these experiments do not include heat transfer from reservoir sediments and/or the advection of heat via the flow of warm fluids, which will both contribute to the thermal budget for dissociation. Permeability was not a dissociation-limiting factor in our experiments, but in a natural setting sediments and dissociation products (especially ice) may undergo compaction deformation in a flowing system, and hence gas release pathways can develop or

(19) Roberts, O. L.; Brownscombe, E. R.; Howe, L. S.; Ramser, H. *Pet. Eng.* **1941**, *12*, 56−62.

be closed off over time. These factors play critical, quite possibly the dominant, roles in gas production scenarios for natural systems. The phase equilibria constraints that dominate in our laboratory experiments are among a number of factors that can govern dynamic natural systems. Such systems may therefore evolve along pathways not encountered in our simplified experiments.

Acknowledgment. We thank George Moridis, Michael Helgerud, and two anonymous reviewers for providing helpful comments during the preparation of the manuscript. We acknowledge the USGS Gas Hydrate Project for providing the resources necessary to do this research.

EF0500437